Geomechanics and Engineering, *Vol. 25, No. 1 (2021) 49-58*
DOI: https://doi.org/10.12989/gae.2021.25.1.049

Surface erosion behavior of biopolymer-treated river sand

Yeong-Man Kwon[1a], Gye-Chun Cho[1b], Moon-Kyung Chung[2c] and Ilhan Chang[*3]

[1]Department of Civil and Environmental Engineering, KAIST, Daejeon 34141, Republic of Korea
[2]Vice President for Research, Korea Institute of Civil Engineering and Building Technology, Goyang-si 10233, Republic of Korea
[3]Department of Civil Systems Engineering, Ajou University, Suwon-si 16499, Republic of Korea

(Received January 25, 2021, Revised March 2, 2021, Accepted March 4, 2021)

Abstract. The resistance of soil to the tractive force of flowing water is one of the essential parameters for the stability of the soil when directly exposed to the movement of water such as in rivers and ocean beds. Biopolymers, which are new to sustainable geotechnical engineering practices, are known to enhance the mechanical properties of soil. This study addresses the surface erosion resistance of river-sand treated with several biopolymers that originated from micro-organisms, plants, and dairy products. We used a state-of-the-art erosion function apparatus with P-wave reflection monitoring. Experimental results have shown that biopolymers significantly improve the erosion resistance of soil surfaces. Specifically, the critical shear stress (i.e., the minimum shear stress needed to detach individual soil grains) of biopolymer-treated soils increased by 2 to 500 times. The erodibility coefficient (i.e., the rate of increase in erodibility as the shear stress increases) decreased following biopolymer treatment from 1 x 10-2 to 1 x 10-6 times compared to that of untreated river-sands. The scour prediction calculated using the SRICOS-EFA program has shown that a height of 14 m of an untreated surface is eroded during the ten years flow of the Nakdong River, while biopolymer treatment reduced this height to less than 2.5 m. The result of this study has demonstrated the possibility of cross-linked biopolymers for river-bed stabilization agents.

Keywords: river-bed terrain; surface erosion; EFA experiment; biopolymer; cross-linking

1. Introduction

Heavy rainfall devastated the Korean Peninsula in August 2020. Reported statistics included 45 deaths, 7,000 flood victims, and the loss of 26,000 ha of agricultural fields. The heavy rainfall resulted in an increase in the amount of fast-flowing water with high shear stress that exceeded the critical shear strength of the adjacent soil. The global detachment process of soils induced by water resulted in water-induced erosion. Local detachment due to soil-structure-water interaction in the vicinity of the ground structure causes scouring (Prendergast and Gavin 2014). Soil erosion and scouring lead to severe damage to river structures including bridges (Deng and Cai 2010), levees (Briaud *et al.* 2008), and dams (Tingsanchali and Chinnarasri 2001). The soil covering (Lauchlan and Melville 2001, Dey and Raikar 2007), flow control (Zarrati *et al.* 2006, Heidarpour *et al.* 2010), and chemical treatments (Bahar *et al.* 2004, Cheng and Cord-Ruwisch 2012) have been applied to mitigate soil erosion induced by water flow.

*Corresponding author, Associate Professor, Ph.D.
E-mail: ilhanchang@ajou.ac.kr
[a]Ph.D. Student
E-mail: yeongman.kwon@kaist.ac.kr
[b]Professor, Ph.D.
E-mail: gyechun@kaist.edu
[c]Senior Research Fellow
E-mail: mkchung@kict.re.kr

Recently, biopolymers, which are microbially induced organic polymers, have been widely attempted as sustainable soil stabilization agents. Previous research has shown that biopolymers can improve the strength (Nugent *et al.* 2010, Chang and Cho 2014, Lee *et al.* 2017, Chang and Cho 2019, Kwon *et al.* 2019, Lee *et al.* 2019), consistency (Chang *et al.* 2019) and reduce the permeability (Bouazza *et al.* 2009, Wiszniewski and Cabalar 2014, Chang *et al.* 2016, Kim *et al.* 2019) of soils. Furthermore, xanthan gum and dextran biopolymers have shown their potential for preventing soil surface erosion by connecting the soil granules, increasing the pore-fluid viscosity, and reducing soil permeability (Ham *et al.* 2018, Kwon *et al.* 2020). Meanwhile, the cross-linking of heterogeneous biopolymers has been studied to increase the molecular weight and improve mechanical properties (Reddy *et al.* 2015). However, more research is needed on the effect of biopolymer cross-linking on erosion prevention.

This study investigates the effects of cross-linked biopolymers on the erosion resistance of river-sands. The erosion function apparatus (EFA) was used to measure the surface erosion of various cross-linked biopolymers. The soil erosion rate (eroded height per hour) was obtained based on P-wave reflection monitoring, and the erosion parameters of critical shear stress and erodibility coefficient were evaluated.

2. Materials and methods

2.1 Soil: Nakdong river-sand

Sand from the Nakdong river was sampled from the

ISSN: 2005-307X (Print), 2092-6219 (Online)

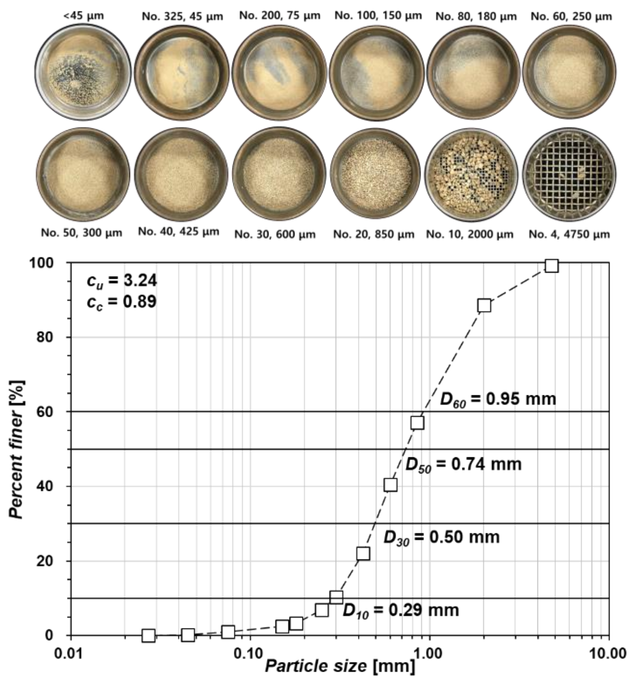

Fig. 1 Particle size distribution and the particle images of Nakdong river-sand used

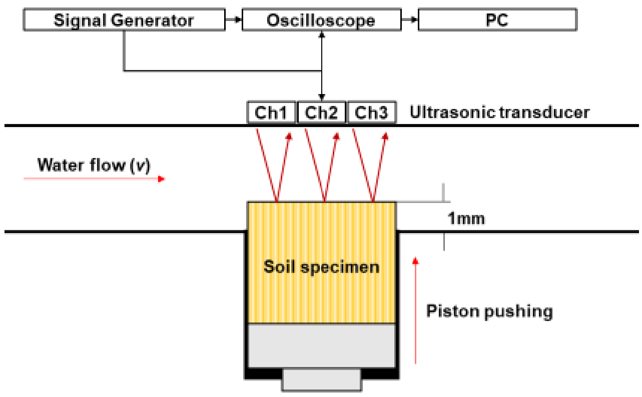

Fig. 2 P-wave sensor embedded erosion function apparatus

Table 1 Sample information for Nakdong river-sand

Treatment	Symbol	m_b/m_s [%]	Water content [%]	Initial void ratio
Untreated	Ref	0	17	0.56
Casein-Xanthan gum	CX	5	12	0.60
Xanthan gum-Starch 1%	XS-1	1	16	0.50
Xanthan gum-Starch 2%	XS-2	2	15	0.53
Starch-Acetic acid- Glycerin	SAG	5	13	0.55

KICT Andong experimental center (36°33’31.8” N 128°33’28.6” E), located near the Nakdong River, in Andong, Korea. Figure 1 shows the particle size distribution of the Nakdong river-sand obtained by a sieve analysis (ASTM 2017) and the particle images remaining on different sizes of sieves. The Nakdong river-sand shows a grain size range of 0.027-4.75 mm, classified as poorly graded sand (SP) with a median diameter (D_{50}) of 0.74 mm. The coefficient of uniformity (C_u) was 3.24, and the coefficient of curvature (C_c) was 0.89. The sampled Nakdong river-sand was dried in an oven at 110 ˚C for 24 h (ASTM 2010).

2.2 Specimen preparation

This study implemented and evaluated the erosion resistance of Nakdong river-sand in an untreated form (referred to in this study as REF) and biopolymer-treated conditions with four different biopolymers. Three different types of mixed biopolymers were used: casein–xanthan gum (CX) using casein (CAS: 9000-71-9) and xanthan gum (CAS: 11138-66-2); xanthan gum–starch (XS) using corn starch (CAS: 9005-25-8); and starch–acetic acid–glycerin (SAG) using corn starch (CAS: 64-19-7) and glycerin (CAS: 56-81-5). The biopolymer combinations have been reported to improve the rheological properties of biopolymer. CX mixtures have been used in the food industry to simultaneously get the characteristics of casein (i.e., emulsion, foam formation, and stability) and xanthan gum (i.e., water-holding and thickening) (Hemar *et al.* 2001). Interaction between starch and xanthan gum showed an increase in the viscosity (Christianson 1981). The addition of glycerin plasticizes the starch, which leads it to be used as biodegradable plastics (Martin *et al.* 2003), while further addition of acid in the glycerin plasticized starch showed an increase in thermal stability, water resistance, and a decrease in retrogradation (Jiugao *et al.* 2005).

Two different biopolymer contents (biopolymer to soil ratio in mass; m_b/m_s =1%, 2%) were chosen for the XS-treated sands (i.e., XS-1 and XS-2) to observe the effect of biopolymer contents on the erosion behavior of river-sands. This study used research-grade biopolymers and chemicals purchased from Merck, Germany. The dry river-sand and biopolymer solutions with a water content of 15% were mixed thoroughly until a uniform biopolymer-treated river-sand mixture was formed. The soil mixtures were then placed into thin-walled tubes each with a length of 300 mm and an inner diameter of 71 mm. Soils were compacted and trimmed to obtain a height of 200 mm. Both ends of the cell were sealed with paraffin to prevent moisture evaporation before the experiments. Table 1 summarizes the specimen details.

2.3 Erosion test using the Erosion Function Apparatus

This study assessed the surface erosion behavior of biopolymer-treated Nakdong river-sand using the erosion function apparatus (EFA) developed by Briaud *et al.* (1999) with the P-wave reflection system implemented by Ham *et al.* (2016). The schematic configuration of the EFA with a P-wave monitoring system is shown in Fig 2. The sample tube was connected to the EFA funnel where a pneumatic piston lifted the sample inside the tube. A steady water flow then saturated the soils. After the saturation process, 1 mm of soil surface was extruded into the funnel and exposed to flowing water. The erosion rate of 1 mm extruded soil surface at various flow velocities (0.12-4.50 m/s) was

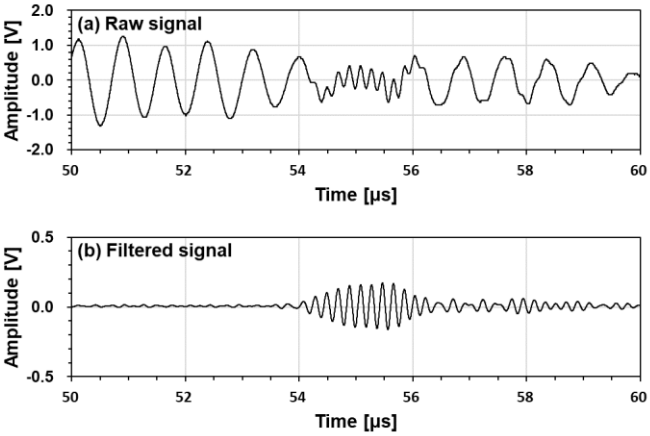

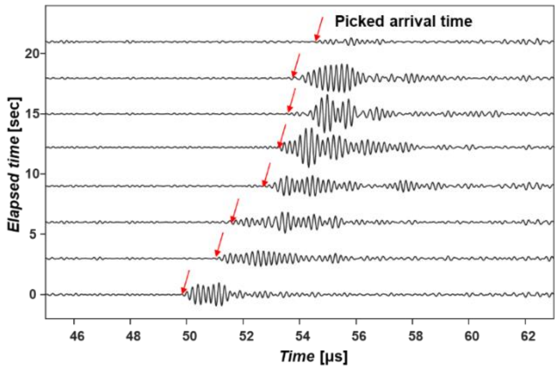

(c) Variation in obtained signals with elapsed time

Fig. 3 P-wave signal analysis

measured and analyzed using P-wave reflections. A source ultrasonic transducer generated input P-waves, and receiver P-wave sensors captured the propagated and reflected P-wave signals. Pencil-type miniature ultrasonic transducers (VP-3, CTS Valpey Co.), with a sensor of 3 mm diameter and 5 mm casing diameter, were used as both source and receiver P-wave sensors. A signal generator (DPR 300, JSR Ultrasonics) was used to generate input P-wave signals. The reflected P-wave signals were recorded using a digital oscilloscope (DSO-X-3024A, Agilent). Three pairs (Ch1, Ch2, and Ch3) of P-wave sensors were installed on the top of the flow funnel with intervals of 25 mm along the flow direction. The reflected P-waves were acquired every 3 seconds.

2.4 Signal analysis

Examples of reflected P-wave signals (for REF exposed to 0.255 m/s of flow velocity) are shown in Fig. 3. To remove unwanted noises from the raw signal (Fig. 3(a)), data reduction has been conducted using a band-pass filter with a cutoff frequency at 1.5 MHz and 4.0 MHz to clarify the signal arrival time as shown in Fig. 3(b). Based on the filtered signals, the arrival times were hand-picked, as shown in Fig. 3(c). Fig. 3(c) also shows the increase in arrival time (i.e., an increase in the travel length of the P-wave signals) with the water flow of constant velocity (0.255 m/s). The eroded height Δz (in mm) was then calculated from the change in arrival time Δt (in seconds), and p-wave velocity in water $V_{p\text{-}water}$ (= 1480 m/s) as:

$$\Delta z = \frac{1}{2} v_{p\text{-}water} (\Delta t) \tag{1}$$

The detailed signal analysis can be found in Ham *et al.* (2016).

2.5 Erosion rate ($\dot{z}$) and shear stress (τ)

The EFA method analyzes the erosion behavior of soils based on the erosion rate $\dot{z}$ and shear stress τ. The $\dot{z}$ (mm/h) is calculated by dividing the erosion depth (1 mm for EFA analysis) by the erosion time for 1 mm erosion t (in seconds) obtained from the P-wave signal analysis as:

$$\dot{z} = \frac{1}{t} \times 3600 \tag{2}$$

The τ (in Pa) is calculated in Eq. (3) based on the mean flow velocity v (in m/s) measured by the flow velocity meter:

$$\tau = \frac{1}{8} f \rho v^2 \tag{3}$$

where f is the friction factor obtained from Moody's chart which varies by the Reynolds number of flowing water (f = 0.030 - 0.038) (Moody 1944), and ρ is the density of water (= 1 g/cm^3). The details of the calculations are given in Briaud *et al.* (2001).

2.6 Critical shear stress, erodibility coefficient, and power exponent

The critical shear stress (τ_c) is defined as the τ where individual soil particles detach and initiate erosion (Briaud *et al.* 1999). This study estimated the τ_c for each specimen from the erosion curve by following the procedure proposed by Briaud *et al.* (2001).

The shape of the erosion function curve (i.e., τ versus $\dot{z}$) follows straight, concave, and convex shapes (Temple 1992, Hanson and Cook 1997, Briaud *et al.* 2001). This study correlates the EFA results based on the power relation between $\dot{z}$ and τ (Ham *et al.* 2018) to reflect various shapes of the erosion curve as:

$$\dot{z} = k_d (\tau - \tau_c)^{\theta} \tag{4}$$

where k_d is the erodibility coefficient (in mm/h/Pa), τ_c is the critical shear stress (in Pa), and θ is the power exponent. The τ_c indicates the minimum τ needed to detach an individual soil particle and initiate soil erosion. The erodibility coefficient and the power function refer to how fast the $\dot{z}$ increases with an increase in τ. The shape of the erosion function curve differs depending on the value of θ: θ < 1 for a concave shape, θ = 1 for a straight shape, and θ > 1 for a convex shape.

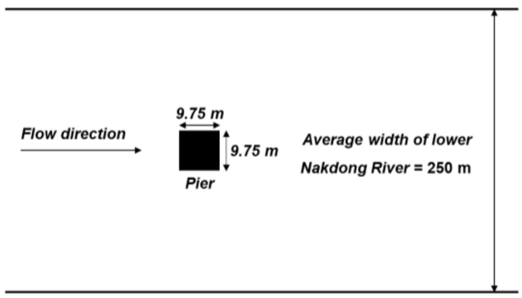

(a) Plan view

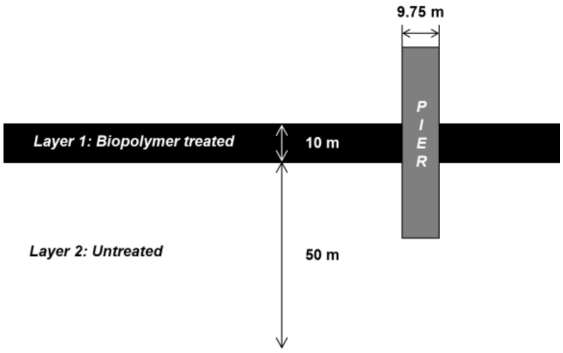

(b) Side view

Fig. 4 Geometry of the pier and channel for SRICOS prediction

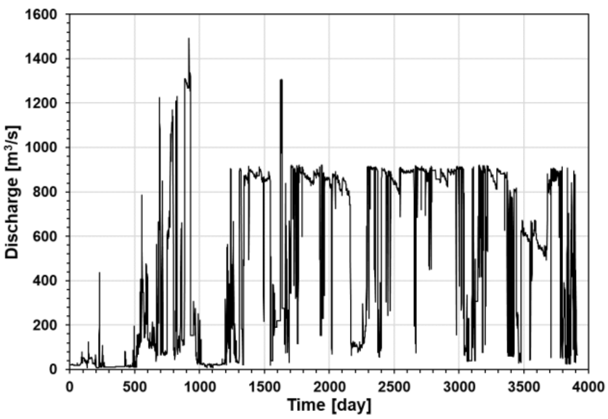

Fig. 5 Hydrograph of Andong bridge from 2010 to 2020

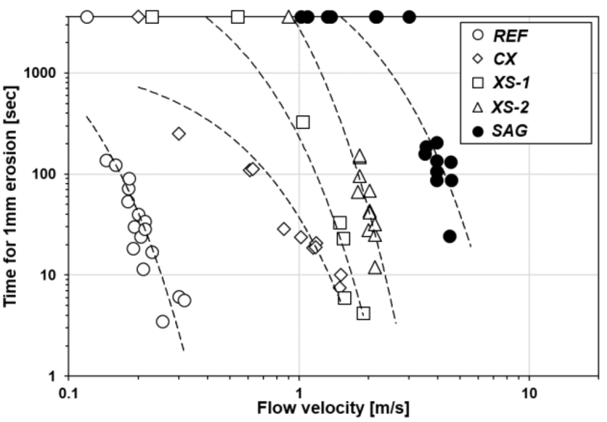

Fig. 6 The variation in the time required for 1 mm erosion of biopolymer treated Nakdong river-sands by flow velocity

2.7 SRICOS-EFA

The prediction of the scour depth while the hydrograph measurements were being taken, was conducted by using the *scour rate in cohesive soil* (SRICOS)–EFA method (Briaud *et al.* 1999).

The erosion function (i.e., τ - $\dot{z}$ relations) obtained on a site-specific basis with the EFA can predict the scour depth versus time curve by using the SRICOS-EFA. The input data for SRICOS-EFA were: 1) the velocity and water depth hydrograph readings, which were converted based on the relationships between discharge–velocity and discharge–water depth; 2) geometry of the pier and channel; and 3) erosion functions of the soil layers.

For SRICOS-EFA analysis, a simple rectangular pier (9.75 m in width × 9.75 m in length) was considered. The upstream channel width was assumed to be 250 m, which is known as the average width of the Nakdong River (Ji *et al.* 2011). The river floor was simulated to compose two layers, where the upper layer becomes a biopolymer-treated soil layer with 10 m thickness and the lower layer with 50 m thickness consisting of untreated soil. Fig. 4 shows a schematic diagram of the analyzed geometry.

The hydrograph data (in terms of discharge; in m^3/s) near the Nakdong River Bridge in Andong, Korea, was obtained from the Water Environment Information System (National Institute of Enviromental Research 2020), as shown in Fig. 5. The average discharge was 499 m^3/s, and the standard deviation was 319 m^3/s.

3. Results

3.1 Time for erosion by flow velocity

The change in the erosion time (i.e., the time required for 1 mm of erosion) with flow velocity is presented in Fig. 6. The average erosion time from the three transducer channels was used to obtain a representative value. Experimental results showed a decrease in the erosion time as the flow velocity increased.

For the untreated soils, to erode 1 mm of soil extrusions, a flow velocity of 0.12 m/s took 3,600 seconds, while a velocity of 0.32 m/s took 3.5 seconds. The $\dot{z}$ was prolonged, and the erosion was not visibly observed at a flow velocity under 0.12 m/s. Erosion seems to start at a flow velocity of approximately 0.12 m/s. The mean velocity of the river was in the range of 0.4–1.5 m/s (Schulze *et al.* 2005). Therefore, it can be postulated that the river-sand used is susceptible to erosion by flowing water if it remains untreated.

Meanwhile, for river-sand treated with biopolymers a significant increase in the flow velocity was required to erode the same amount (1 mm) of soil within the same time. These results are shown graphically in Fig. 6. Comparing the results for XS-1 and XS-2 indicates that erosion resistance improves with a higher biopolymer content, and the SAG resists to the highest flow velocity among the specimen observed.

3.2 Erosion curve

Fig. 7 depicts the erosion curve (i.e., the variation in $\dot{z}$

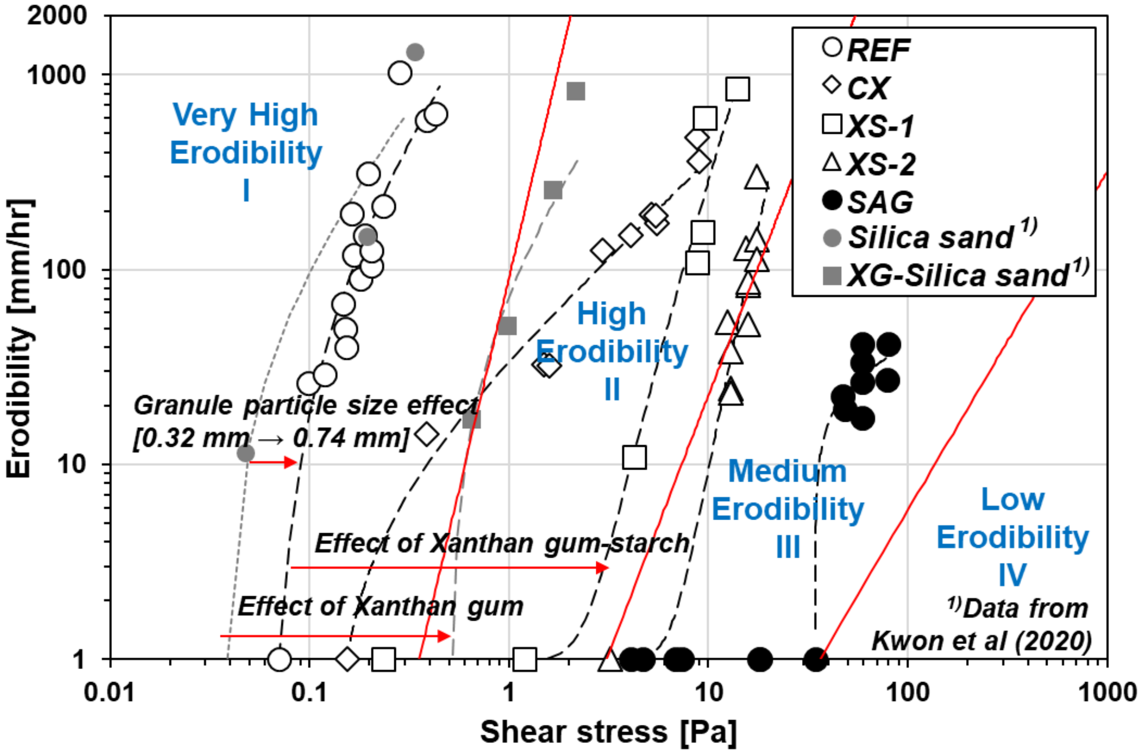

Fig. 7 Erosion curves of biopolymer treated river-sands

Table 2 Erosion parameters of Nakdong river-sand

Symbol	Critical shear stress [Pa]	Erodibility coefficient [mm/hr/Pa]	Power exponent	Class
Ref	0.07	3913.60	1.55	Very High Erodibility [I]
CX	0.15	38.21	0.99	Very High Erodibility [I] - High Erodibility [II]
XS-1	1.19	0.32	3.11	High Erodibility [II]
XS-2	3.21	0.0049	3.89	High Erodibility [II] – Medium Erodibility [III]
SAG	34.44	7.84	0.39	Medium Erodibility [III]

with τ increase) compared with previous EFA results on xanthan gum-treated silica sand with a mean diameter of 0.32 mm (Kwon *et al.* 2020). Comparison with previous data was conducted to examine the reliability of the experimental results of this study, the effect of particle size on the erosion behavior, and the effect of biopolymer crosslinking. The experimental results were modeled using the data with a τ higher than the τ_c and an $\dot{z}$ faster than 1 mm/h based on Eq. (4). For the overall specimen, the $\dot{z}$ increased with higher τ, while the erosion curve showed both convex (REF, XS-1, XS-2) and concave (CX, and SAG) shapes.

When comparing the silica and untreated Nakdong river-sands, the Nakdong river-sand showed a higher erosion resistance than the silica sand. In detail, silica sand showed a τ_c of 0.036 Pa, while that of the Nakdong river-sand was 0.070 Pa. The Nakdong river-sand with a larger mean diameter (D_{50} = 0.74 mm) showed higher resistance to flowing water than the silica sand (D_{50} = 0.32 mm), because the erosion resistance of cohesionless soils is known to show a linear relationship with the particle diameter (Briaud *et al.* 1999).

Biopolymer treatments were found to reduce the $\dot{z}$ for any given τ. The untreated soils eroded by $\dot{z}$ of over 10 mm/h even at a τ of 0.1 Pa. Meanwhile, all biopolymer-treated specimens showed prolonged erosion (under 1 mm/h) at a τ of 0.1 Pa. XS-1 and XS-2 soils showed a higher erosion resistance than the CX soils. In contrast, the variation in $\dot{z}$ due to τ was higher than that of CX-treated soils. Thus, the difference of $\dot{z}$ between CX and XS-1 became smaller as τ increased.

A higher XS concentration (XS-2) resulted in higher resistance to flowing water compared to the XS-1. It is noted that the shear strength of biopolymer treated soils peaked at a certain biopolymer content (Chang and Cho 2019). Thus, a further study on the optimal biopolymer content for erosion prevention is required. Furthermore, XS-1 showed a more significant variation in the erosion curve than the 1% xanthan gum treated silica sand compared to untreated sands, which showed that the mixing of different biopolymers could further enhance soil erosion resistance. The SAG-treated river-sands showed the most significant increase in τ required to erode sands with similar $\dot{z}$ among the specimen observed.

3.3 Comparison of erosion parameters

Table 2 and Fig. 8 summarize the results of the data reduction following Eq. (4). The τ_c was estimated from the test results by following the procedure suggested by Briaud

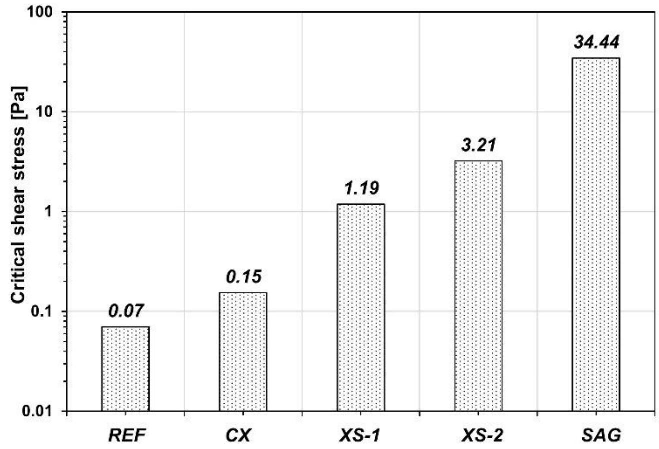

Fig. 8 The variation in the critical shear stress of biopolymer treated river-sands

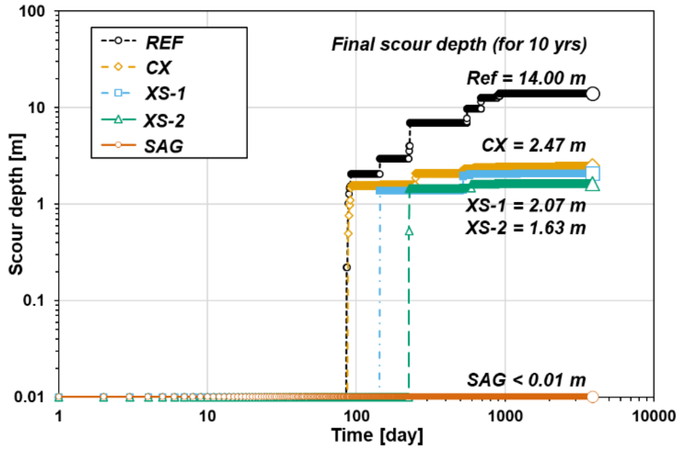

Fig. 9 Scour depth predicted by SRICOS during 10 years

et al. (2001). Then, the parameters k and θ were calculated based on the curve fitting of erosion curves where the $\tau > \tau_c$, and $\dot{z}$ > 1mm/hr. The τ_c is related to the soil particle to particle contact, particle size, and the forces between soil particles (Briaud *et al.* 2001). The untreated Nakdong river-sand showed a τ_c of 0.07 Pa, which is near the lower limit of previously reported τ (0.05-0.42 Pa) at which the sandy river bed can be exposed (Biron *et al.* 2004). Lower τ_c of REF than τ acting on the river-bed indicates that further stabilization of river-sand is essential for the stability of river-structures.

As expected, biopolymer treatment resulted in a significant increase in erosion resistance (i.e., higher τ_c, lower k_d) of the soils. Fig. 8 shows that biopolymer treatment resulted in a 2 (CX) to 500 (SAG) times higher τ_c than for the untreated specimen (REF). Based on the erosion resistance classes referred from Briaud (2008), untreated Nakdong river-sand is in the range of "very high erodibility (I)". However, the CX and XS-1 treatment enhanced it to a "high erodibility (II)" level, and XS-2 showed resistance in the boundary of "high erodibility (II)" to "medium erodibility (III)". While SAG raised it further to "medium erodibility (III)", which is the same category as a jointed rock with spacing less than 30 mm, low plasticity clays.

The erodibility coefficient (k_d) is defined as the $\dot{z}$ of soils at a low τ level (i.e., $\dot{z}$ *at* $\tau = \tau_c + 1$). The value indicates how fast the $\dot{z}$ increases with τ. As shown in Table 2, the biopolymer treatment significantly reduced the erodibility coefficient of the Nakdong river-sand. The erodibility coefficient of biopolymer-treated sand decreased by from 1 × 10^{-2} to 1 × 10^{-6} over untreated sand, which shows that the biopolymer treated river-sands are less susceptible to the variation in the shear stress.

The power exponent indicates the variation of the $\dot{z}$ with the τ higher than the τ_c, which is related to the erosion mechanism (Briaud *et al.* 2001). In the case of XS, the erosion mechanism seems to change from particle-to-particle detachment at low τ levels to block-by-block erosion at higher τ levels, which resulted in a higher $\dot{z}$ at high τ (convex shape). Because viscous XS hydrogels in pore-space aggregates sand particles, aggregate-by-aggregate erosion occurs when the τ becomes sufficiently high to detach aggregates.

However, SAG fills void spaces by forming a plasticized SAG solid (Curvelo *et al.* 2001). Thus, water seems to mainly flow through the interface between SAG and sand particles, where the strength appears weaker than that of the SAG plastics. Therefore, individual particle grains eroded, which leads to the concave shape of the erosion curve.

4. Discussions

4.1 Scour prediction

The EFA experiments were conducted with a constant velocity. However, the flow velocity, in reality, varies frequently, as shown in Fig. 4. Thus, the scour prediction based on the temporal variations of flow velocity was conducted based on the SRICOS-EFA method. The SRICOS scour estimation results are plotted in Fig. 9. Fig. 9 can be compared to the measured hydrograph in Fig. 5. As can be seen, biopolymer treatment has significantly mitigated the entire erosion process. Soil samples excluding SAG reached the final scour depth before 1,000 days, and the scour depth was slightly varied after the 1,000th day because the discharge (1,492 m^3/s) peaked at the 919th day.

Untreated Nakdong river-sand reached an erosion depth of 1 m on the first 88th day (Mar. 29th, 2010) when discharge increased from 22 m^3/s to 45 m^3/s. Meanwhile, 91 (Apr. 1st, 2010), 144 (May. 24th, 2010), and 227 (Aug. 15th, 2010) days were required to erode the same depth (1 m) for CX, XS-1, and XS-2, where the discharge reached 80 m^3/s, 124 m^3/s, and 195 m^3/s, respectively. In comparison, the SAG-treated soils have scoured depth within 0.01 m throughout the observation period.

Additionally, the final scour depth was significantly reduced with biopolymer treatment. Untreated soil eroded up to 13.99 m on the 919th day (Jul. 7th, 2012), which was the third heavy rainfall season (discharge of 1500 m^3/s). Meanwhile, biopolymer-treated layers (10 m in depth) were not entirely eroded in all cases. In other words, biopolymers resulted in over 82% reduction (0.01-2.47 m) on the final scour depth compared to REF (13.99 m). In datils, CX finally eroded by 2.47 m at 2247th day with a discharge of 110 m^3/s, XS-1 reached 2.07 m at 1198th date with a discharge of 318 m^3/s, and XS-2 reached 1.63 m at 854th date with a discharge of 635 m^3/s. Lastly, the SAG-treated sample showed no erosion during the ten years of water flow because the recorded discharge did not reach the τ_c of SAG (34.44 Pa). The results for the simple SRICOS prediction have shown the potentials of biopolymer treatment as river-bed stabilization agents.

The scour prediction in this study is performed under the assumption of an ideal situation where biopolymers are evenly dispersed to a depth of 10 m, and there is no change in biopolymer performance over a long period of time. In reality, biodegradable characteristics of biopolymers possibly weaken the biopolymer matrix in soils (Lucas *et al.* 2008, Chang *et al.* 2017). Besides, the distribution of biopolymer in the field may be more heterogeneous than prepared in a laboratory. Therefore, a further study is required by considering the heterogeneity during biopolymer treatment in the field and the durability of the biopolymers.

4.2 Possible mechanisms for erosion resistance

This experimental study shows that soil reinforcement by mixing various biopolymers enhances soil surface resistance to water flow. The reinforcement of the soil surface via biopolymer treatment can be explained by four possible mechanisms related to the mechanical properties of biopolymer, particle contact conditions, and the chemical properties of pore spaces.

First, the cross-linking of biopolymers can improve the mechanical properties of biopolymer molecules. A previous study conducted by Reddy and Yang (2010) showed that the cross-linking of starch with citric acid showed a two-fold increase in the tensile strength of biopolymer molecules by forming cross-linked starch films. The tensile strength of the biopolymer itself can improve the resistance of biopolymers to water flow-induced shear stress. Additionally, Reddy and Yang (2010) showed that the biopolymer cross-linking reduced the accessible regions on its molecular surface and decreased the weight loss of biopolymers in the water media from 75% to 25% after ten days in water. The improvement in the resistance of biopolymers to water dissolution by cross-linking resulted in higher resistance to the erosion induced by the flowing water. Thus, the XS treated river-sand have shown the larger variation in the erosion fuction, compared to the silica sands treated with xanthan gum solely (Fig. 7).

Second, biopolymers enhance the soil particle contact by biopolymer interaction and inter-particle bonds formation (Renault *et al.* 2009, Khatami and O'Kelly 2012, Chang *et al.* 2015). The enhancement of particle contact increased the shear strength and compressive strength (Chen *et al.* 2019), increasing erosion resistance. Furthermore, the critical shear strength of soils is mainly governed by particle bonding because it directly affects the grain contact. In SAG treated river-sands, the highest critical shear stress was observed because the solidified SAG strongly bonds sand grains.

Third, CX and XS biopolymers form a viscous hydrogel that is known to increase the shear strength of soils (Nugent *et al.* 2009). The higher shear strength possibly resulted in the higher erosion resistance of soils. Furthermore, the viscosity of pore-fluids can suppress particle movement as a viscous fluid damper (Fujino *et al.* 1992) that causes the delay in the erosion progress when the τ exceeds the τ_c of the soil surface (i.e., reduction in the k_d). The cross-linkage of biopolymers can further improve the erosion resistance of soil surface via enhancing the viscosity of biopolymers. Christianson (1981) and Kim and Yoo (2006) have shown that starch modification by mixing xanthan gum enhances pore-fluid viscosity via molecular interactions between starch and xanthan gum.

Lastly, the biopolymer solution clogs the intergranular pore spaces which reduces water infiltration or hydraulic conductivity (El-Morsy *et al.* 1991, Chang *et al.* 2015). Previous studies showed biopolymer treatment reducing soil permeability by an order of 100 or greater (Martin *et al.* 1996, Chang *et al.* 2016). The lower permeability resulted in a decrease in the seepage flow, which is nontrivial for surface erosion (Ham *et al.* 2018).

5. Conclusions

This study aims to assess the effect of biopolymers on the surface erosion resistance of coarse-grained river-sand to flowing water. Several biopolymers (i.e., xanthan gum, corn starch, casein, and acetic acid) are mixed with Nakdong river-sand. The surface erosion functions of each specimen were assessed using an erosion function apparatus (EFA) with a P-wave monitoring system installed. It is essential to stabilize the soil surface from surface erosion by flowing water because the safety of bed structures such as levees, dams, and foundations are dependent on it. Furthermore, the scouring behavior by river water flows was predicted using the SRICOS-EFA program considering the ten-years hydrograph database of the Nakdong River. The experimental results have shown that biopolymer treatment enhances the erosion resistance of river-sands. The critical shear stress (i.e., the minimum shear stress needed to initiate detachment of the individual soil particles) increased from 2 (Casein-xanthan gum mixture; CX) to 500 (Starch-acetic acid-glycerin mixture; SAG) times.

Additionally, biopolymers have reduced the erodibility coefficient (i.e., the initial variation in the erosion rate) by a factor of from 1×10^{-2} (CX) to 1×10^{-6} (XS-2) in time compared to that of untreated sands. Meanwhile, the XS biopolymers form viscous hydrogels and aggregate particles, which eroded block-by-block resulting in faster erosion at high shear stress levels (i.e., high power exponent). The predicted eroded depth caused by the ten years of the Nakdong River flows significantly reduced the scour depth from 14 m (REF) to < 0.01 m (SAG), as estimated from the erosion function results. The possible mechanisms of biopolymer treatment can be hypothesized as follows: 1) enhancement of the mechanical properties of biopolymers by cross-linking, 2) enhancement of sand particle contact by the biopolymer, 3) suppression of particle movement due to the viscosity of the biopolymer solution, and 4) the reduction in the permeability of soils via pore-clogging by the biopolymers.

The results of this study showed the potential of biopolymer cross-linking for the stabilization of river surface treatment. The validation of the cross-linking mechanism on various types of soils has not yet been completed. A further step is to analyze the cross-linking biopolymer effect on the fine-grained soils that have surface charge characteristics.

Acknowledgments

The research described in this paper was financially supported by Korea Ministry of Land, Infrastructure and Transport (MOLIT) as the Water Management Research Program (21AWMP-B114119-06).

References

ASTM (2010), D2216-10: Standard test methods for laboratory determination of water (moisture) content of soil and rock by mass, ASTM International, West Conshohocken, Pennsylvania, U.S.A.

ASTM (2017), D6913/D6913M-17: Standard test methods for particle-size distribution (gradation) of soils using sieve analysis, ASTM International, West Conshohocken, Pennsylvania, U.S.A.

Bahar, R., Benazzoug, M. and Kenai, S. (2004), "Performance of compacted cement-stabilised soil", *Cement Concrete Compos.*, **26**(7), 811-820. https://doi.org/10.1016/j.cemconcomp.2004.01.003.

Biron, P.M., Robson, C., Lapointe, M.F. and Gaskin, S.J. (2004), "Comparing different methods of bed shear stress estimates in simple and complex flow fields", *Earth Surf. Proc. Land.*, **29**(11), 1403-1415. https://doi.org/10.1002/esp.1111.

Bouazza, A., Gates, W. and Ranjith, P. (2009), "Hydraulic conductivity of biopolymer-treated silty sand", *Géotechnique*, **59**(1), 71-72. https://doi.org/10.1680/geot.2007.00137.

Briaud, J.L. (2008), "Case histories in soil and rock erosion: Woodrow wilson bridge, brazos river meander, normandy cliffs, and new orleans levees", *J. Geotech. Geoenviron. Eng.*, **134**(10), 1425-1447. https://doi.org/10.1061/(ASCE)1090-0241(2008)134:10(1425).

Briaud, J.L., Chen, H.C., Govindasamy, A.V. and Storesund, R. (2008), "Levee erosion by overtopping in new orleans during the Katrina hurricane", *J. Geotech. Geoenviron. Eng.*, **134**(5), 618-632. https://doi.org/10.1061/(ASCE)1090-0241(2008)134:5(618).

Briaud, J.L., Ting, F., Chen, H., Gudavalli, R., Kwak, K., Philogene, B., Han, S.W., Perugu, S., Wei, G. and Nurtjahyo, P.J.T.T.I. (1999), *SRICOS: Prediction of Scour Rate at Bridge Piers*, Texas A&M University, C.S., Texas, U.S.A., 2937-293.

Briaud, J.L., Ting, F.C.K., Chen, H.C., Gudavalli, R., Perugu, S. and Wei, G. (1999), "SRICOS: Prediction of scour rate in cohesive soils at bridge piers", *J. Geotech. Geoenviron. Eng.*, **125**(4), 237-246. https://doi.org/10.1061/(ASCE)1090-0241(1999)125:4(237).

Briaud, J.L., Ting, F.C.K., Chen, H.C., Cao, Y., Han, S.W. and Kwak, K.W. (2001), "Erosion function apparatus for scour rate predictions", *J. Geotech. Geoenviron. Eng.*, **127**(2), 105-113. https://doi.org/10.1061/(ASCE)1090-0241(2001)127:2(105).

Chang, I. and Cho, G.C. (2014), "Geotechnical behavior of a beta-1,3/1,6-glucan biopolymer-treated residual soil", *Geomech. Eng.*, **7**(6), 633-647. https://doi.org/10.12989/gae.2014.7.6.633.

Chang, I. and Cho, G.C. (2019), "Shear strength behavior and parameters of microbial gellan gum-treated soils: From sand to clay", *Acta Geotechnica*, **14**(2), 361-375. https://doi.org/10.1007/s11440-018-0641-x.

Chang, I., Im, J. and Cho, G.C. (2016), "Geotechnical engineering behaviors of gellan gum biopolymer treated sand", *Can. Geotech. J.*, **53**(10), 1658-1670. https://doi.org/10.1139/cgj-2015-0475.

Chang, I., Im, J., Lee, S.W. and Cho, G.C. (2017), "Strength durability of gellan gum biopolymer-treated Korean sand with cyclic wetting and drying", *Constr. Build. Mater.*, **143**, 210-221. https://doi.org/10.1016/j.conbuildmat.2017.02.061.

Chang, I., Im, J., Prasidhi, A.K. and Cho, G.C. (2015), "Effects of xanthan gum biopolymer on soil strengthening", *Constr. Build. Mater.*, **74**, 65-72. https://doi.org/10.1016/j.conbuildmat.2014.10.026.

Chang, I., Kwon, Y.M., Im, J. and Cho, G.C. (2019), "Soil consistency and interparticle characteristics of xanthan gum biopolymer-containing soils with pore-fluid variation", *Can. Geotech. J.*, **56**(8), 1206-1213. https://doi.org/10.1139/cgj-2018-0254.

Chang, I., Prasidhi, A.K., Im, J., Shin, H.-D. and Cho, G.-C. (2015), "Soil treatment using microbial biopolymers for anti-desertification purposes", *Geoderma*. **253-254**, 39-47. https://doi.org/10.1016/j.geoderma.2015.04.006.

Chen, C., Wu, L., Perdjon, M., Huang, X. and Peng, Y. (2019), "The drying effect on xanthan gum biopolymer treated sandy soil shear strength", *Constr. Build. Mater.*, **197**, 271-279. https://doi.org/10.1016/j.conbuildmat.2018.11.120.

Cheng, L. and Cord-Ruwisch, R. (2012), "In situ soil cementation with ureolytic bacteria by surface percolation", *Ecol. Eng.*, **42**, 64-72. https://doi.org/10.1016/j.ecoleng.2012.01.013.

Christianson, D.D. (1981), "Gelatinization of wheat starch as modified by xanthan gum, guar gum, and cellulose gum", *Cereal Chem.*, **58**(6), 513-517.

Curvelo, A.A.S., de Carvalho, A.J.F. and Agnelli, J.A.M. (2001), "Thermoplastic starch-cellulosic fibers composites: Preliminary results", *Carbohyd. Polym.*, **45**(2), 183-188. https://doi.org/10.1016/S0144-8617(00)00314-3.

Deng, L. and Cai, C.S. (2010), "Bridge scour: Prediction, modeling, monitoring, and countermeasures", *Practice Period. Struct. Des. Construct.*, **15**(2), 125-134. https://doi.org/10.1061/(ASCE)SC.1943-5576.0000041.

Dey, S. and Raikar, R.V. (2007), "Clear-water scour at piers in sand beds with an armor layer of gravels", *J. Hydraul. Eng.*, **133**(6), 703-711. https://doi.org/10.1061/(ASCE)0733-9429(2007)133:6(703).

El-Morsy, E.A., Malik, M. and Letey, J. (1991), "Polymer effects on the hydraulic conductivity of saline and sodic soil conditions", *Soil Sci.*, **151**(6), 430-435.

Fujino, Y., Sun, L., Pacheco, B.M. and Chaiseri, P. (1992), "Tuned liquid damper (TLD) for suppressing horizontal motion of structures", *J. Eng. Mech.*, **118**(10), 2017-2030. https://doi.org/10.1061/(ASCE)0733-9399(1992)118:10(2017).

Ham, S.M., Chang, I., Noh, D.H., Kwon, T.H. and Muhunthan, B. (2018), "Improvement of surface erosion resistance of sand by microbial biopolymer formation", *J. Geotech. Geoenviron. Eng.*, **144**(7), 06018004. https://doi.org/10.1061/(ASCE)GT.1943-5606.0001900.

Ham, S., Kwon, T., Chang, I. and Chung, M. (2016), "Ultrasonic P-wave reflection monitoring of soil erosion for erosion function apparatus", *Geotech. Test. J.*, **39**(2), 301-314. https://doi.org/10.1520/GTJ20150040.

Hanson, G. and Cook, K. (1997), "Development of excess shear stress parameters for circular jet testing", *ASAE Paper*, **972227**.

Heidarpour, M., Afzalimehr, H. and Izadinia, E. (2010), "Reduction of local scour around bridge pier groups using collars", *Int. J. Sediment Res.*, **25**(4), 411-422. https://doi.org/10.1016/S1001-6279(11)60008-5.

Hemar, Y., Tamehana, M., Munro, P.A. and Singh, H. (2001), "Viscosity, microstructure and phase behavior of aqueous mixtures of commercial milk protein products and xanthan gum", *Food Hydrocolloid.*, **15**(4), 565-574. https://doi.org/10.1016/S0268-005X(01)00077-7.

Ji, U., Julien, P.Y. and Park, S.K. (2011), "Sediment flushing at the Nakdong River estuary barrage", *J. Hydraul. Eng.*, **137**(11), 1522-1535. https://doi.org/10.1061/(ASCE)HY.1943-7900.0000395.

Jiugao, Y., Ning, W. and Xiaofei, M. (2005), "The effects of citric acid on the properties of thermoplastic starch plasticized by glycerol", *Starch Stärke*. **57**(10), 494-504. https://doi.org/10.1002/star.200500423.

Khatami, H.R. and O'Kelly, B.C. (2012), "Improving mechanical properties of sand using biopolymers", *J. Geotech. Geoenviron. Eng.*, **139**(8), 1402-1406. https://doi.org/10.1061/(ASCE)GT.1943-5606.0000861.

Kim, C. and Yoo, B. (2006), "Rheological properties of rice starch-xanthan gum mixtures", *J. Food Eng.*, **75**(1), 120-128. https://doi.org/10.1016/j.jfoodeng.2005.04.002.

Kim, Y.M., Park, T. and Kwon, T.H. (2019), "Engineered bioclogging in coarse sands by using fermentation-based bacterial biopolymer formation", *Geomech. Eng.*, **17**(5), 485-496. https://doi.org/10.12989/gae.2019.17.5.485.

Kwon, Y.M., Chang, I., Lee, M. and Cho, G.C. (2019), "Geotechnical engineering behaviors of biopolymer-treated soft marine soil", *Geomech. Eng.*, **17**(5), 453-464. https://doi.org/10.12989/gae.2019.17.5.453.

Kwon, Y.M., Ham, S.M., Kwon, T.H., Cho, G.C. and Chang, I. (2020), "Surface-erosion behaviour of biopolymer-treated soils assessed by EFA", *Géotechnique Lett.*, **10**(2), 1-7. https://doi.org/10.1680/jgele.19.00106.

Lauchlan, C.S. and Melville, B.W. (2001), "Riprap protection at bridge piers", *J. Hydraul. Eng.*, **127**(5), 412-418. https://doi.org/10.1061/(ASCE)0733-9429(2001)127:5(412).

Lee, S., Chang, I., Chung, M.K., Kim, Y. and Kee, J. (2017), "Geotechnical shear behavior of xanthan gum biopolymer treated sand from direct shear testing", *Geomech. Eng.*, **12**(5), 831-847. https://doi.org/10.12989/gae.2017.12.5.831.

Lee, S., Im, J., Cho, G.C. and Chang, I. (2019), "Laboratory triaxial test behavior of xanthan gum biopolymer-treated sands", *Geomech. Eng.*, **17**(5), 445-452. https://doi.org/10.12989/gae.2019.17.5.445.

Lucas, N., Bienaime, C., Belloy, C., Queneudec, M., Silvestre, F. and Nava-Saucedo, J.E. (2008), "Polymer biodegradation: Mechanisms and estimation techniques – A review", *Chemosphere*. **73**(4), 429-442. https://doi.org/10.1016/j.chemosphere.2008.06.064.

Martin, G., Yen, T. and Karimi, S. (1996), "Application of biopolymer technology in silty soil matrices to form impervious barriers", *Proceedings of the 7th Australia New Zealand Conference on Geomechanics: Geomechanics in a Changing World*, Adelaide, Australia, July.

Martin, O., Averous, L. and Della Valle, G. (2003), "In-line determination of plasticized wheat starch viscoelastic behavior: Impact of processing", *Carbohyd. Polym.*, **53**(2), 169-182. https://doi.org/10.1016/S0144-8617(03)00040-7.

Moody, L.F. (1944), "Friction factors for pipe flow", *Trans. ASME*, **66**, 671-684.

National Institute of Enviromental Research (2020), *Water Environment Information System*.

Nugent, R.A., Zhang, G. and Gambrell, R.P. (2009), "Effect of exopolymers on the liquid limit of clays and its engineering implications", *Transport. Res. Rec.*, **2101**(1), 34-43. https://doi.org/10.3141/2101-05.

Nugent, R.A., Zhang, G. and Gambrell, R.P. (2010), "The effects of exopolymers on the erosional resistance of cohesive sediments", *Proceedings of the International Conference on Scour and Erosion (ICSE-5) 2010*, San Francisco, California, U.S.A., November.

Prendergast, L.J. and Gavin, K. (2014), "A review of bridge scour monitoring techniques", *J. Rock Mech. Geotech. Eng.*, **6**(2), 138-149. https://doi.org/10.1016/j.jrmge.2014.01.007.

Reddy, N., Reddy, R. and Jiang, Q. (2015), "Crosslinking biopolymers for biomedical applications", *Trends Biotechnol.*, **33**(6), 362-369. https://doi.org/10.1016/j.tibtech.2015.03.008.

Reddy, N. and Yang, Y. (2010), "Citric acid cross-linking of starch films", *Food Chem.*, **118**(3), 702-711. https://doi.org/10.1016/j.foodchem.2009.05.050.

Renault, F., Sancey, B., Badot, P.M. and Crini, G. (2009), "Chitosan for coagulation/flocculation processes–An eco-friendly approach", *Eur. Polym. J.*, **45**(5), 1337-1348. https://doi.org/10.1016/j.eurpolymj.2008.12.027.

Schulze, K., Hunger, M. and Döll, P. (2005), "Simulating river flow velocity on global scale", *Adv. Geosci.*, **5**, 133-136.

Temple, D.M. (1992), "Estimating flood damage to vegetated deep soil spillways", *Appl. Eng. Agric.*, **8**(2), 237-242. https://doi.org/10.13031/2013.26059.

Tingsanchali, T. and Chinnarasri, C. (2001), "Numerical modelling of dam failure due to flow overtopping", *Hydrolog. Sci.*, **46**(1), 113-130. https://doi.org/10.1080/02626660109492804.

Wiszniewski, M. and Cabalar, A.F. (2014), *Hydraulic conductivity of a Biopolymer Treated Sand*, in *New Frontiers in*

Geotechnical Engineering, 19-27.
Zarrati, A.R., Nazariha, M. and Mashahir, M.B. (2006), “Reduction of local scour in the vicinity of bridge pier groups using collars and riprap”, *J. Hydraul. Eng.*, **132**(2), 154-162. https://doi.org/10.1061/(ASCE)0733-9429(2006)132:2(154).

IC